Calculation of UV attenuation and colored dissolved organic matter absorption spectra from measurements of ocean color

S. C. Johannessen[1]
Institute of Ocean Sciences, Contaminant Chemistry, North Saanich, British Columbia, Canada

W. L. Miller and J. J. Cullen
Department of Oceanography, Dalhousie University, Halifax, Nova Scotia, Canada

Received 27 June 2000; revised 22 August 2001; accepted 24 February 2003; published 25 September 2003.

[1] The absorption of ultraviolet and visible radiation by colored or chromophoric dissolved organic matter (CDOM) drives much of marine photochemistry. It also affects the penetration of ultraviolet radiation (UV) into the water column and can confound remote estimates of chlorophyll concentration. Measurements of ocean color from satellites can be used to predict UV attenuation and CDOM absorption spectra from relationships between visible reflectance, UV attenuation, and absorption by CDOM. Samples were taken from the Bering Sea and from the Mid-Atlantic Bight, and water types ranged from turbid, inshore waters to the Gulf Stream. We determined the following relationships between in situ visible radiance reflectance, L_u/E_d (λ) (sr^{-1}), and diffuse attenuation of UV, $K_d(\lambda)$ (m^{-1}): $K_d(323nm) = 0.781[L_u/E_d(412)/L_u/E_d(555)]^{-1.07}$; $K_d(338nm) = 0.604[L_u/E_d(412)/L_u/E_d(555)]^{-1.12}$; $K_d(380\ nm) = 0.302[L_u/E_d(412)/L_u/E_d(555)]^{-1.24}$. Consistent with published observations, these empirical relationships predict that the spectral slope coefficient of CDOM absorption increases as diffuse attenuation of UV decreases. Excluding samples from turbid bays, the ratio of the CDOM absorption coefficient to K_d is 0.90 at 323 nm, 0.86 at 338 nm, and 0.97 at 380 nm. We applied these relationships to SeaWiFS images of normalized water-leaving radiance to calculate the CDOM absorption and UV attenuation in the Mid-Atlantic Bight in May, July, and August 1998. The images showed a decrease in UV attenuation from May to August of approximately 50%. We also produced images of the areal distribution of the spectral slope coefficient of CDOM absorption in the Georgia Bight. The spectral slope coefficient increased offshore and changed with season. *INDEX TERMS:* 4552 Oceanography: Physical: Ocean optics; 4850 Oceanography: Biological and Chemical: Organic marine chemistry; 4275 Oceanography: General: Remote sensing and electromagnetic processes (0689); *KEYWORDS:* remote sensing, SeaWiFS, colored dissolved organic matter, diffuse attenuation of downwelling radiation, K_d, ultraviolet radiation

Citation: Johannessen, S. C., W. L. Miller, and J. J. Cullen, Calculation of UV attenuation and colored dissolved organic matter absorption spectra from measurements of ocean color, *J. Geophys. Res.*, *108*(C9), 3301, doi:10.1029/2000JC000514, 2003.

1. Introduction

[2] Colored or chromophoric dissolved organic matter in the ocean is a strong absorber of ultraviolet radiation and the precursor for many photochemical reactions. Photochemical oxidation of colored dissolved organic matter (CDOM), may explain the hitherto unknown fate of a large portion of the terrestrially derived dissolved organic carbon that enters the ocean [*Kieber et al.*, 1989; *Mopper et al.*, 1991]. Its photochemical products include dissolved inorganic carbon, DIC (CO_2, HCO_3^-, and CO_3^{-2}); [*Chen et al.*, 1978; *Miles and Brezonik*, 1981; *Allard et al.*, 1994; *Vähätalo et al.*, 2000; *Miller and Zepp*, 1995; *Granéli et al.*, 1996; *Moore*, 1999], CO [*Kettle*, 1994; *Valentine and Zepp*, 1993], H_2O_2 [*Sikorski and Zika*, 1993a, 1993b; *Miller and Kester*, 1994; *Moore et al.*, 1993], $OH^\bullet$ [*Zhou and Mopper*, 1990; *Mopper and Zhou*, 1990], oxygen radicals [*Cooper et al.*, 1989; *Blough and Zepp*, 1995], and many small, biologically labile organic molecules [*Bushaw et al.*, 1996; *Moran and Zepp*, 1997].

[3] Since CDOM is responsible for much of the attenuation of ultraviolet radiation (UV) in the ocean [*Bricaud et al.*, 1981], changes in the spectral CDOM absorption coefficient, a_{CDOM},(λ) can change the depth of penetration of UV. This is of interest to biologists, because UV is known to inhibit phytoplankton productivity [*Cullen and Neale*, 1994] and to damage bacteria [*Jeffrey et al.*, 1996; *Kaiser and Herndl*, 1997; *Jeffrey et al.*, 2000].

[1]Formerly at Department of Oceanography, Dalhousie University, Halifax, Nova Scotia, Canada.

0148-0227/03/2000JC000514$09.00

Absorbance by CDOM at visible wavelengths can also interfere with estimates of chlorophyll concentration made from remotely sensed data [*Carder et al.*, 1989; *Michaels and Siegel*, 1996]. To evaluate all these processes quantitatively, it is essential to know the shape and magnitude of the CDOM absorption spectrum, which varies widely among locations and seasons [*Michaels and Siegel*, 1996; *Højerslev*, 1998].

[4] A number of researchers have developed algorithms to relate remotely sensed properties to in situ absorption or fluorescence by CDOM or to the concentration of dissolved organic carbon, DOC [*Fenton et al.*, 1994; *Vodacek et al.*, 1995; *Ferrari et al.*, 1996]. *Hochman et al.* [1994] and *Hoge et al.* [1995] used the water-leaving radiance at 443 nm calculated from CZCS (Coastal Zone Color Scanner) data together with an assumed CDOM absorption spectral slope coefficient to determine a_{CDOM} in situ. *Kahru and Mitchell* [2001] used a ratio of SeaWiFS (Sea-viewing Wide Field-of-view Sensor) normalized water-leaving radiance at 443 and 510 nm to calculate a_{CDOM} at 300 nm, which they suggested could be used with an assumed spectral slope to calculate the full absorption spectrum.

[5] In addition to the CZCS channels, SeaWiFS has a detector for upwelling radiance at 412 nm. One of the reasons for including this sensor was to facilitate remote estimates of dissolved organic matter [*Nelson*, 1997]. Here, we present empirically derived relationships that make use of measurements at 412 nm to allow the accurate calculation of $a_{CDOM}(\lambda)$, the slope coefficient of the a_{CDOM} spectrum, and UV attenuation from remotely sensed reflectance data, without the assumption of a single spectral shape for the CDOM absorption spectrum.

2. Methods

2.1. Approach

[6] *Austin and Petzold* [1981] showed that the diffuse attenuation coefficient for downwelling visible irradiance, $K_d(\lambda)$ (m^{-1}), could be estimated from the ratio of the upwelling radiance, $L_u(\lambda)$, at two wavelengths measured by CZCS. The wavelength ratio approach is also applied to the prediction of chlorophyll concentration in surface waters [*Gordon et al.*, 1983; *Aiken et al.*, 1992], and images of global ocean chlorophyll concentrations and $K(490)$ are now produced routinely from SeaWiFS data (SeaWiFS Project, http://seawifs.gsfc.nasa.gov/SEAWIFS.html (verified 12 May 2000)). SeaWiFS does not have UV detectors; atmospheric interference makes direct satellite measurements of UV upwelling radiance from the ocean extremely difficult. However, it seems reasonable to apply the reflectance ratio method to the UV, since the components of seawater which absorb UV radiation also absorb visible radiation.

[7] To produce synoptic estimates of a_{CDOM} (λ) and of photochemical production rates from remotely sensed data, *Cullen et al.* [1997] suggested an approach in several steps which would make use of the 412 nm sensor: (1) relate satellite measurements of water-leaving radiance to in situ radiance reflectance, defined as the ratio of upwelling radiance to downwelling irradiance; (2) find empirical relationships between the ratio of reflectance at two visible wavelengths (412 nm and 555 nm) and K_d at several UV wavelengths; (3) calculate spectrally resolved total UV absorption from $K_d(UV)$; (4) determine the magnitude of absorption by particles, particularly phytoplankton; (5) subtract absorption due to particles and water from the total to calculate the CDOM absorption; and (6) apply an action spectrum to calculate photochemical production. The estimates of absorption and attenuation could be combined with measurements or estimates of surface irradiance to calculate absorption by CDOM as a function of depth. We modified the *Cullen et al.* [1997] approach by finding direct, empirical relationships between $K_d(UV)$ and a_{CDOM} at corresponding wavelengths rather than calculating a_{CDOM} by difference.

2.2. Sample Locations

[8] Four cruises were undertaken in the Mid-Atlantic Bight in the summers of 1996, 1997, and 1998 and one in the Bering Sea in June 1997. Sample locations are shown in Figure 1. During the July 1997 cruise aboard the *R/V Seward Johnson*, optical casts were made at five stations along cross-shelf transects. Optical casts were made aboard the *R/V Cape Henlopen* in May and August 1997 and in July 1998 at 11, 24, and 37 stations, respectively. In the Bering Sea aboard the R/V *Wecoma*, optical casts were made at 13 stations along a cross-shelf transect.

2.3. Sample Collection and Storage

[9] At each station water was collected from the surface, and at many stations samples were also collected from below the mixed layer using a CTD rosette. Water samples were filtered to remove particles, including bacteria; during the first Mid-Atlantic Bight cruise in 1997, samples were filtered on board through Whatman GF/F (nominal pore size 0.7 μm) filters and then refiltered through 0.2 μm Schleicher and Schuell Nylon 66 membrane filters on return to the lab. Water taken during the other cruises was immediately filtered through 0.2 μm Schleicher and Schuell Nylon 66 filters. During the August 1997 cruise, samples were pressure-filtered using a peristaltic pump with a 0.2 μm in-line filter; samples from the other cruises were vacuum-filtered. Water samples were stored for less than a year in the dark at 4°C in amber glass bottles to minimize biological activity and photochemical breakdown of CDOM. Related studies on seawater have shown no measurable change in absorption at 350 nm over three months of storage under these conditions: measurements of CDOM absorption made on 0.2-μm-filtered water from the Suwannee River in Georgia showed no measurable change in absorbance after at least three years of storage (W. L. Miller, unpublished data, 1995); water filtered through GF/F filters, stored for up to three months and then refiltered through 0.2 μm filters was found to have the same absorption coefficient at 350 and 440 nm as water filtered through 0.2 μm filters and measured immediately (S. C. Johannessen, unpublished data, 1997).

2.4. Absorption Measurements

[10] Spectral absorption was measured in a 10 cm quartz flow cell in a Hewlett Packard HP 8453 diode array spectrophotometer, blanked against Barnstead Nanopure UV-treated distilled water. Spectral absorption, $A_{CDOM}(\lambda)$ (dimensionless) was measured from 190 nm to 1100 nm,

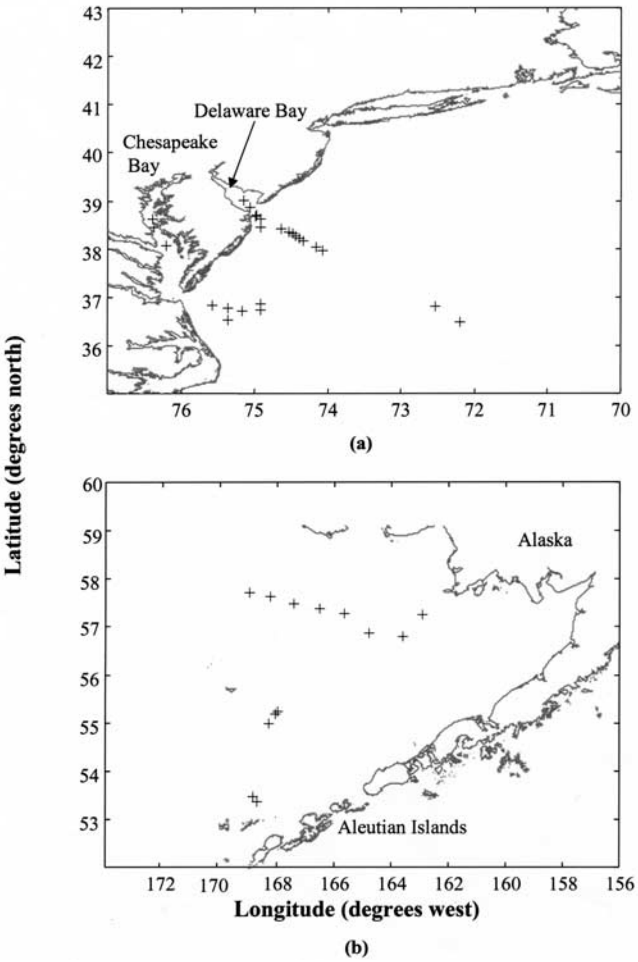

Figure 1. Sample locations. (a) Mid-Atlantic Bight, July 1996, May and August 1997, and July 1998; (b) Bering Sea, June 1997.

and the values were converted to absorption coefficient, $a_{CDOM}(\lambda)$ (m^{-1}), according to the relation:

$$a_{CDOM}(\lambda) = 2.303\ A_{CDOM}(\lambda)/l \qquad (1)$$

[*Miller*, 1997] where l is the path length of the spectrophotometer cell (m). Table 1 lists the symbols and abbreviations used in this paper. Scattering by fine particles, blank drift (in single beam spectrophotometers), and a difference between the index of refraction of the seawater sample and of the distilled water blank can all affect the measured spectral absorption. Instead of correcting for each problem individually, an equation was fit to the absorption spectra to solve for an offset (a_0) at higher wavelengths where CDOM absorption decreases to zero:

$$a_{CDOM}(\lambda) = C\mathrm{e}^{-S\lambda} + a_0 \qquad (2)$$

Each absorption spectrum was fit to this relationship over the range 280–550 nm, where C (m^{-1}) and a_0 (m^{-1}), and S (nm^{-1}) were determined by nonlinear least squares regression. The parameter S is the slope coefficient of CDOM absorption. The offset, a_0, was then subtracted from the whole spectrum to correct a_{CDOM} for the offset. (The offset was always less than 7% of the absorption coefficient at 300 nm and less than 14% of that at 350 nm.) The fit was not used for any purpose other than to provide an offset value for the correction of $a_{CDOM}(\lambda)$.

[11] This subtraction, like other commonly used constant offset corrections of CDOM absorption spectra, assumes that the scattering, blank drift and difference in the index of refraction are all independent of wavelength, an assumption which may not be valid for scattering by very fine particles. The use of an equation of this form to fit CDOM absorption data has been described by *Markager and Vincent* [2000], *Stedmon et al.* [2000], *Johannessen* [2000] and *Johannessen and Miller* [2001].

2.5. In Situ Radiometric Measurements

[12] Two instruments were deployed at each optical station. A Satlantic SeaWiFS Profiling Multichannel Radiometer (SPMR) measured downwelling irradiance at depth in twelve channels (2 nm bandwidth for UV, 10 nm for visible channels; acquisition rate 6 Hz) centered on the following wavelengths: 305 (UVB), 323 (UVA/UVB boundary), 338 (UVA), 380 (UVA), 412, 443, 490, 510, 532, 555, 670, 683, and 700 nm. The visible channels coincided with those of the radiance sensors on the SeaWiFS satellite (SeaWiFS Project, http://seawifs.gsfc.nasa.gov/SEAWIFS.html (verified 12 May 2000); Satlantic Inc., http://www.satlantic.com/ (updated 2000 and verified 12 May 2000), although the SeaWiFS bandwidth was wider (20 nm for 412–555 nm; 40 nm for 670–700 nm). The diffuse attenuation coefficient for downwelling irradiance was calculated over the first optical depth (from the surface to the depth at which the downwelling irradiance fell to 1/e of its surface value) using a statistical fit to the irradiance data with the Matlab® routine "ksurf " (written and provided by R.F. Davis, Dalhousie Univ.). The routine made use of the relationship:

$$K_d(\lambda, z + 1/2\Delta z) = ln(E_d(\lambda, z)/E_d(\lambda, z + \Delta z))/\Delta z \qquad (3)$$

[*Kirk*, 1994] where $E_d(\lambda, z)$ ($Wm^{-2}\ nm^{-1}$) is downwelling irradiance measured at the first depth, $E_d(\lambda, z + \Delta z)$ is the downwelling irradiance at the subsequent depth, and Δz is the change in depth, z (m), between two consecutive measurements (typically about 12 cm). The standard deviation of K_d measurements at UV and blue wavelengths, based on replicate profiles, ranged from 2% for open ocean stations to 6% for inshore stations. (Replicate profiles help to assess the error in the Kd estimate introduced by wave focusing [*Zaneveld et al.*, 2001]). Profiles were dark-corrected using the dark calibration values determined at the Satlantic Inc. calibration laboratory prior to and following each cruise. Deviations from dark values in situ have little effect on estimates of K_d in the first optical depth, except at short wavelengths (in this case 323 nm), where the limit of detection may be reached within the first optical depth at some stations.

[13] A Satlantic Ocean Color Radiometer, OCR, simultaneously measured incident downwelling irradiance just above the ocean's surface in the same thirteen wave bands as the profiler and also at 590 nm. It provided a surface reference for the profiler's irradiance measurements to correct for changes in incident irradiance, $E_d(\lambda, 0^+)$, during

Table 1. Notation

Variable	Definition
$a(\lambda)$	Total spectral absorption coefficient (m^{-1})
a_0	Spectrophotometric absorption coefficient offset (m^{-1})
$a_{CDOM}(\lambda)$	Spectral absorption coefficient of CDOM (m^{-1})
$a_{CDOM(fit)}(\lambda)$	Spectral absorption coefficient of CDOM (m^{-1}) calculated from the statistical fit used to determine the spectrophotometric offset
$a_{CDOM(spec)}(\lambda)$	Spectral absorption coefficient of CDOM (m^{-1}) calculated from $A_{CDOM}(\lambda)$ and not yet corrected for spectrophotometric offset
$A_{CDOM}(\lambda)$	Spectral absorption by CDOM measured in spectrophotometer (dimensionless)
$b(\lambda)$	Total spectral scattering (m^{-1})
C	Constant in absorption coefficient correction equation (m^{-1})
CDOM	Colored or chromophoric dissolved organic matter
D	Julian day (January 1 = 1)
DIC	Dissolved inorganic carbon
e	Eccentricity of the Earth's orbit around the Sun (dimensionless)
$E_d(\lambda)$	Incident (downwelling) spectral irradiance (W m^{-2} nm^{-1} or moles photons m^{-2} s^{-1})
$E_d(\lambda, 0^+)$	Incident (downwelling) spectral irradiance just above the surface of the ocean (W m^{-2} nm^{-1} or moles photons m^{-2} s^{-1})
$E_d(\lambda, z)$	Incident (downwelling) spectral irradiance at depth (W m^{-2} nm^{-1} or moles photons m^{-2} s^{-1})
$F_o(\lambda)$	Mean extraterrestrial spectral solar irradiance corrected for Earth-Sun distance and orbital eccentricity (W m^{-2} nm^{-1})
$H_o(\lambda)$	Mean extraterrestrial solar spectral irradiance (W m^{-2} nm^{-1})
$K_d(\lambda)$	Spectral diffuse attenuation coefficient for downwelling irradiance (m^{-1})
λ	Wavelength (nm)
l	Path length (m) in a spectrophotometer
$L_u(\lambda, 0^-)$	Upwelling spectral radiance just below the surface of the ocean (W m^{-2} nm^{-1} sr^{-1})
$L_u(\lambda)/E_d(\lambda)$	Spectral radiance reflectance (sr^{-1})
$L_w(\lambda, 0^+)$	Upwelling (water-leaving) spectral radiance just above the surface of the ocean (W m^{-2} nm^{-1} sr^{-1})
$\bar{\mu}_d(\lambda)$	Average cosine of downwelling irradiance (dimensionless)
$nL_w(\lambda)$	Normalized water-leaving spectral radiance (W m^{-2} nm^{-1} sr^{-1})
S	Slope coefficient of CDOM absorption (nm^{-1})
S_{Kd}	Slope coefficient of K_d (nm^{-1})
SeaWiFS	Sea-viewing Wide Field-of-view Sensor
UV	Ultraviolet radiation
z	Depth (m)

the profile. The OCR also measured upwelling radiance just below the water's surface (depth ranged from 0 to 15 cm below the surface) in the same fourteen channels. Radiance reflectance (sr^{-1}) was calculated as the ratio of upwelling radiance, $L_u(\lambda, 0^-)$ (Wm^{-2} nm^{-1} sr^{-1}) just below the surface, to downwelling irradiance, $E_d(\lambda, 0^+)$ (Wm^{-2} nm^{-1}) just above the surface [from *Kirk*, 1994]:

$$Radiance\ reflectance(\lambda) = Lu(\lambda, 0^-)/E_d(\lambda, 0^+) \tag{4}$$

3. Results

3.1. Calculation of $K_d(\lambda)$ From Reflectance

[14] The diffuse attenuation coefficient for downwelling irradiance at each of 323, 338 and 380 nm was plotted against several ratios of visible reflectance to find the strongest correlation. Of the ratios tried, the ratio of reflectance at 412 nm to reflectance at 555 nm predicted K_d at 323, 338, and 380 nm most robustly (Figure 2). (Although by convention the y axis is reserved for the dependent variable, the purpose of the plot was to find an equation that could be used to predict K_d from reflectance.) For clarity, error bars (see "Methods" section) are omitted from Figure 2. Reflectance at 412 nm alone predicted K_d at 323, 338 and 380 nm fairly well for those stations outside of the very turbid Delaware and Chesapeake Bays (data not shown). However, the $L_u/E_d(412)/L_u/E_d(555)$ ratio allowed the inclusion of all stations in a single relationship. Regressions on these data yielded the following empirical relationships (n = 53):

$$K_d(323\text{nm}) = 0.781[L_u/E_d(412)/L_u/E_d(555)]^{-1.07} \quad r^2 = 0.91 \tag{5}$$

$$K_d(338\text{nm}) = 0.604[L_u/E_d(412)/L_u/E_d(555)]^{-1.12} \quad r^2 = 0.91 \tag{6}$$

$$K_d(380\text{nm}) = 0.302[L_u/E_d(412)/L_u/E_d(555)]^{-1.24} \quad r^2 = 0.95 \tag{7}$$

3.2. Calculation of CDOM Absorption Coefficient From K_d

[15] CDOM is thought to be responsible for most of the UV attenuation in the ocean [*Bricaud et al.*, 1981]. To determine the proportion of $K_d(UV)$ due to CDOM, and to investigate how that proportion varied with location, measured a_{CDOM} was plotted against measured K_d at corresponding wavelengths for all stations (Figure 3). K_d predicts a_{CDOM} well at 323 and 338 nm, and reasonably well at 380 nm; the correlation breaks down at longer wavelengths where other components, particularly phyto-

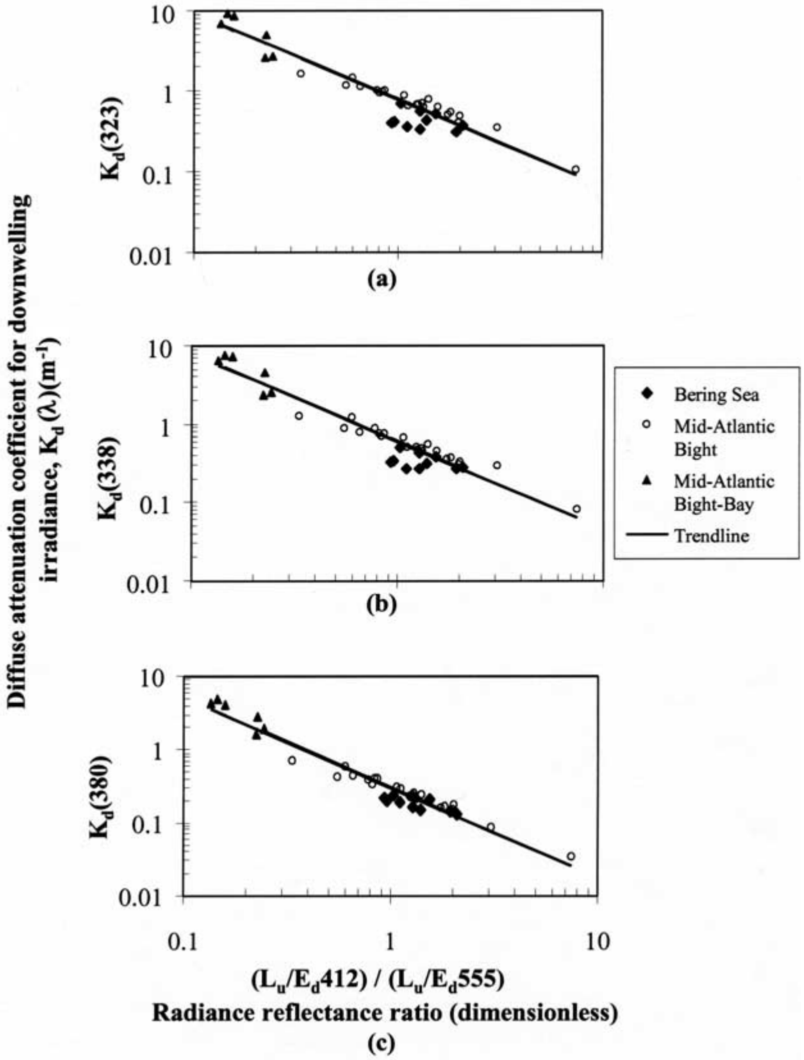

Figure 2. In situ diffuse attenuation coefficient for downwelling irradiance at three UV wavelengths versus the ratio of in situ reflectances at 412 and 555 nm (n = 53) on a log-log scale. Trend lines represent equations (5)–(7) in the text.

plankton pigments, absorb more strongly. K_d and a_{CDOM} seem to be related linearly. The following regression equations were determined for water taken from a wide variety of environments—from coastal to off shelf, blue waters in the Bering Sea and from the coast to the Gulf Stream in the Mid-Atlantic Bight (n = 33):

$$a_{CDOM}(323) = 0.904\ K_d(323) - 0.00714;\quad r^2 = 0.93 \qquad (8)$$

$$a_{CDOM}(338) = 0.858\ K_d(338) - 0.0190;\quad r^2 = 0.92 \qquad (9)$$

$$a_{CDOM}(380) = 0.972\ K_d(380) - 0.0171;\quad r^2 = 0.66 \qquad (10)$$

Table 2 gives 95% confidence intervals for the slope coefficients and intercepts given in equations (8)–(13). The intercept values above are within the uncertainty of the absorption measurements, and Table 2 shows that 0 is well within their 95% confidence intervals. This suggests that at each UV wavelength, CDOM absorption contributes a constant proportion of attenuation. (A small negative intercept is consistent with contributions to absorption from other sources.) We found that the six samples from inside the turbid Delaware and Chesapeake Bays did not fit the above relationships. However, while the number of bay samples was too low to give convincing statistics, the plots of a_{CDOM} versus K_d for these samples were also strikingly linear (Figure 3 inset). The equations of the best fit regression lines to the bay data are:

$$a_{CDOM}(323) = 0.308\ K_d(323) + 0.0463;\quad r^2 = 0.97;\ n = 5 \qquad (11)$$

$$a_{CDOM}(338) = 0.259\ K_d(338) + 0.171;\quad r^2 = 0.94; n = 6 \qquad (12)$$

$$a_{CDOM}(380) = 0.183\ K_d(380) + 0.400;\quad r^2 = 0.97; n = 5 \qquad (13)$$

[16] The lower proportion of K_d attributable to CDOM inside the bays probably results from absorption of UV by

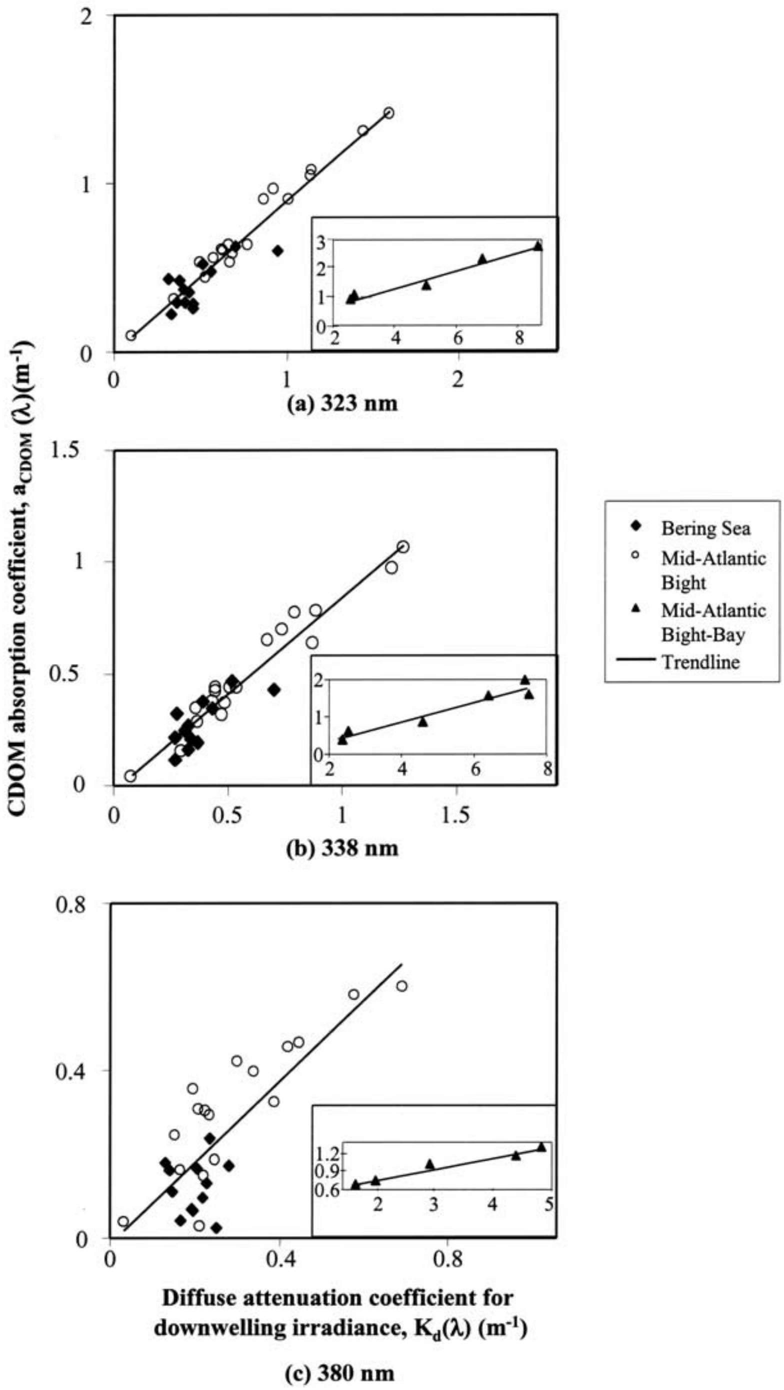

Figure 3. Absorption coefficient of CDOM versus in situ diffuse attenuation coefficient for downwelling irradiance at three UV wavelengths (n = 33). "Bay" data from Delaware and Chesapeake Bays are inset. Trend lines represent equations (8)–(13) in the text. See Table 2 for confidence intervals.

organic or organically coated particles and from increased particle backscattering.

3.3. Calculation of K_d and CDOM Absorption Coefficient From Satellite Data

[17] The empirical relationships described in equations (5)–(7) were applied to three SeaWiFS archive data scenes to evaluate their use as predictors of K_d. The satellite data were level 3, monthly binned images with 9 × 9 km resolution from May, July, and August 1998. The satellite was not operational during the 1996 and 1997 cruises, but the July 1998 image includes the period of the last cruise.

[18] Images of normalized water-leaving radiance at 412 and 555 nm from the Distributed Active Archive Center (from the August–September 1998 reprocessing; http://daac.gsfc.nasa.gov/(updated 10 May 2000 and verified 12 May 2000)), were used to calculate a reflectance ratio (L_u/E_d (412)/L_u/E_d (555)) at each pixel as described below.

Table 2. Coefficients and Confidence Intervals for Relationships Between a_{CDOM} and K_d at Three UV Wavelengths for Offshore (n = 33) and Bay (n = 6) Samples[a]

	Slope Coefficient	Slope Lower 95% CL	Slope Upper 95% CL	Intercept	Intercept Lower 95% CL	Intercept Upper 95% CL
			323 nm			
Offshore	0.904	0.809	0.998	−0.00712	−0.0771	0.0628
Bay	0.308	0.203	0.414	0.0463	−0.556	0.648
			338 nm			
Offshore	0.858	0.760	0.956	−0.0190	−0.0751	0.0370
Bay	0.259	0.167	0.351	−0.171	−0.682	0.340
			380 nm			
Offshore	0.972	0.699	1.25	−0.0171	−0.0964	0.0622
Bay	0.183	0.121	0.244	0.400	0.191	0.610

[a]See equations (8)–(13) in the text and Figure 3.

Normalized water leaving radiance, nL_w ($\mathrm{Wm^{-2}\,nm^{-1}\,sr^{-1}}$), is related to water-leaving radiance, $L_w(0^+)$ ($\mathrm{Wm^{-2}\,nm^{-1}\,sr^{-1}}$), by the following equation (modified from *Fraser et al.* [1997]):

$$nL_w = L_w(0^+)(F_o/E_d(0^+)) \tag{14}$$

where F_o is mean extraterrestrial solar irradiance corrected for Earth-Sun distance and orbital eccentricity ($\mathrm{Wm^{-2}\,nm^{-1}}$), and E_d (0^+) is downwelling irradiance measured just above the surface of the ocean ($\mathrm{Wm^{-2}\,nm^{-1}}$). (The wavelength dependence of the variables is left implicit to simplify the equations.) Since the OCR reference measures upwelling radiance just below the surface of the ocean, $L_u(0^-)$ ($\mathrm{Wm^{-2}\,nm^{-1}\,sr^{-1}}$), was calculated from $L_w(0^+)$, according to *Gordon and Clark* [1981]:

$$L_w(0^+) = \sim 0.57\ L_u(0^-) \tag{15}$$

Substituting for $L_w(0^+)$ in equation (14), the ratio of water-leaving radiance at 412 nm to that at 555 nm was related to the ratio of the measurable, in situ reflectance at those wavelengths:

$$\frac{nL_w(412)}{nL_w(555)} = \frac{0.57\ F_0(412)L_u(412,0^-)/E_d(412,0^+)}{0.57\ F_0(555)L_u(555,0^-)/E_d(555,0^+)} \tag{16}$$

$F_o(412)$ and $F_o(555)$ were calculated according to *Gordon et al.* [1983].

$$F_o(\lambda) = H_o(\lambda)(1 + e\ \cos(2\ \pi\ (D-3)/365))^2 \tag{17}$$

where $H_o(\lambda)$ is the mean extraterrestrial solar irradiance ($\mathrm{Wm^{-2}\,nm^{-1}}$), and e is the eccentricity of the Earth's orbit (0.0167) [*Gordon et al.*, 1983]. *Gregg and Carder* [1990] give the following values for $H_o(\lambda)$:

$$H_o(412) = 1.812\ \mathrm{Wm^{-2}nm^{-1}}$$

$$H_o(555) = 1.896\ \mathrm{Wm^{-2}nm^{-1}}$$

[19] Using the empirical relationships described in earlier sections of this paper and the reflectance ratio L_u/E_d (412)/ L_u/E_d (555) calculated from the SeaWiFS normalized water-leaving radiance values at each pixel, K_d and a_{CDOM} were calculated at 323, 338 and 380 nm. Figure 4 shows maps of calculated K_d at 323 nm for May, July, and August 1998 in the Mid-Atlantic Bight. SeaWiFS images are unreliable in areas with high concentrations of particles in the water [*Kahru and Mitchell*, 1999], because the algorithm used to calculate $nL_w(412)$ relies on the assumption that all the radiation at 670 nm incident on the surface of the water is absorbed [*Fraser et al.*, 1997]. That assumption is not valid in areas of high particle concentration. The problem is often manifested in negative nearshore $nL_w(412)$ values. For this study, an arbitrary cutoff value of 2.0×10^{-3} $\mathrm{Wm^{-2}\,nm^{-1}\,sr^{-1}}$ was chosen, and all pixels with $nL_w(412)$ or $nL_w(555)$ below that value were masked. Masked pixels are shown in black in Figure 4, as is land. (Of course, the in situ measurements of reflectance at 412 nm are not subject to atmospheric interference, so they provide a way to ground truth the satellite measurements.)

[20] While most of the in situ data were collected before the SeaWiFS satellite was operational, values of K_d measured at 323, 338, and 380 nm at three stations during the July 1998 cruise compared well with those calculated at the nearest pixel from the monthly binned, July 1998 SeaWiFS image (Table 3). The stations were chosen to represent midshelf, shelf break and offshelf waters. We also compared K_d values determined in August 1997 in the Gulf Stream with those calculated for the nearest pixel in August 1998 (Table 3). The modeled K_d at 323 nm was within 10% of the measured value at each station. The modeled values of K_d at 338 and 380 nm were within 30% of the measured values at the midshelf station and within 6% in the Gulf Stream. At the midshelf and shelf break stations the modeled K_d values were all higher than the actual values, probably as a result of problems with the atmospheric correction in the presence of particles or of a high concentration of CDOM (as explained above).

[21] A K_d slope coefficient was calculated for each station, using an exponential regression on the three UV K_d values both modeled and determined in situ (Table 3; Figure 5). The K_d values calculated in equations (5)–(7) are not independent of one another; they can be derived from one another by rearranging the equations, and thus the equations specify one slope coefficient for each reflectance ratio. In fact, the slope coefficient for $K_d(\lambda)$ is almost exactly described by the relationship, S_{Kd} = 0.0166 + 0.00674 log(Lu/Ed(412)/Lu/Ed(555)), as shown in Figure 5. There is a unique slope for every magnitude of K_d at a given wavelength. The slope coefficient determined for each

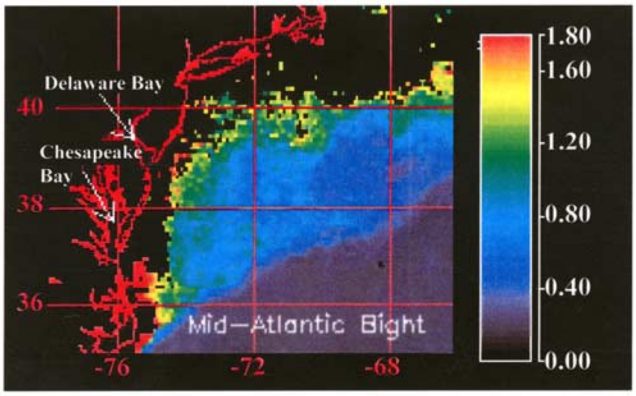

(a) May, 1998

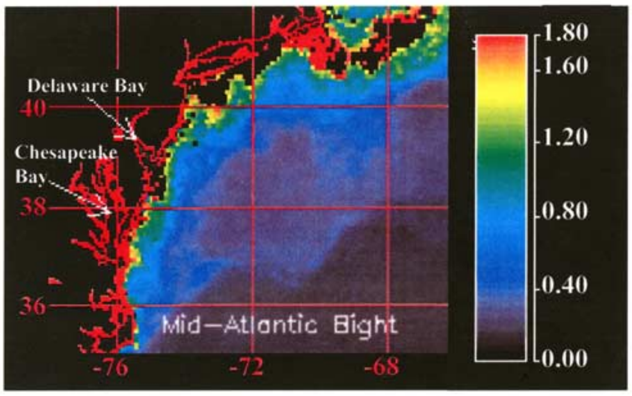

(b) July, 1998

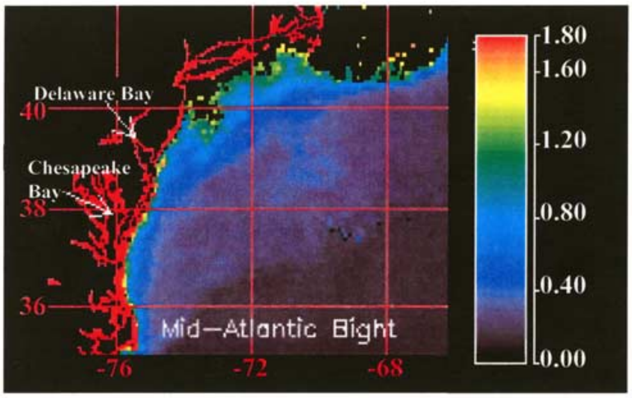

(c) August, 1998

Figure 4. Diffuse attenuation coefficient for downwelling irradiance (m^{-1}) at 323 nm in the Mid-Atlantic Bight, calculated from SeaWiFS normalized water-leaving radiance data, binned to 9 km × 9 km, monthly resolution: (a) May 1998, (b) July 1998, and (c) August 1998.

9 km × 9 km bin using the modeled K_d values was within 20% of that determined from the in situ K_d values at the station in the same area. Clearly, the relationships presented above give a good estimate of UV attenuation in the ocean.

[22] We applied the relationships presented in equations (5)–(10) to produce an image of the areal distribution

Table 3. Comparison of K_d Values Determined in Situ and Calculated From a SeaWiFS Ocean Color Image[a]

Station	Station Location	Satellite Image Pixel Location	In Situ R 412/R 555	Modeled R 412 / R 555	%R Diff. (Model − In Situ)/In Situ	Wavelength, nm	In Situ K_d, m^{-1}	Modeled K_d, m^{-1}	% K_d Diff. (Model − In Situ)/In Situ	In Situ K_d Slope Coeff., nm^{-1}	Modeled K_d Slope Coeff., nm^{-1}	% Slope Coeff. Difference (Model − In Situ)/In Situ
M9807-7	38.36°N, 74.47°W	38.26°N, 74.43°W	0.827	0.672	−19	323	1.09	1.20	9	0.0155	0.0178	15
						338	0.722	0.942	31			
						380	0.380	0.494	30			
M9807-37	38.00°N, 74.04°W	37.85°N, 74.03°W	1.91	1.70	−11	323	0.405	0.444	10	0.0182	0.0185	2
						338	0.279	0.334	20			
						380	0.138	0.157	14			
M9807-14	37.12°N, 72.93°W	36.84°N, 73.03°W	2.27	1.78	−22	323	0.446	0.422	−6	0.0229	0.0183	−20
						338	0.324	0.317	−2			
						380	0.122	0.148	21			
M9708-15	36.02°N, 72.29°W	36.33°N, 72.23°W	7.46	6.29	−16	323	0.105	0.109	3	0.0200	0.0215	8
						338	0.0797	0.0770	−3			
						380	0.0338	0.0319	−6			

[a]For the M9807 stations, both the measurements and the satellite image were taken in July 1998. The K_d values for station M9708-15 (Gulf Stream) were calculated from in situ measurements in August 1997 and from a satellite image of August 1998.

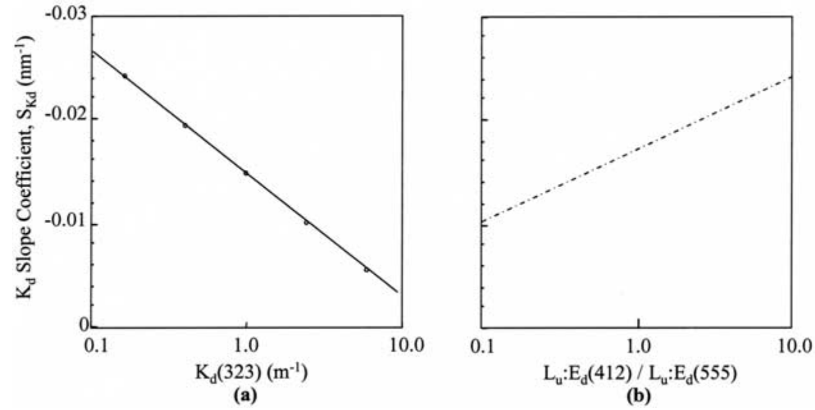

Figure 5. (a) Slope coefficient of the diffuse attenuation coefficient versus diffuse attenuation coefficient at 323 nm. The regression equation is $S_{Kd} = 0.0159 - 0.00632 \log(K_d(323))$; $r^2 = 0.9997$. (b) Slope coefficient of the diffuse attenuation coefficient versus the ratio of $L_u(412)/E_d(412)$ to $L_u(555)/E_d(555)$. The regression equation is $S_{Kd} = 0.0166 + 0.00674 \log(L_u{:}E_d(412)/L_u{:}E_d(555))$; $r^2 = 0.9997$. Both plots show the monotonic increase in the slope coefficient as attenuation decreases and reflectance increases. The trend is consistent with published observations.

of the CDOM absorption slope coefficient in the Georgia Bight in January and July 1999 (Figure 6) from SeaWiFS archive images. The slope coefficients are based on the CDOM absorption coefficient at 323 and 338 nm. (SeaDAS, the program used to make the image, does not do nonlinear regressions.) Pixels where the normalized water-leaving radiance at 412 nm is unreliable, as described for Figure 4, are masked in black.

[23] Using equations (5)–(10), calculated a_{CDOM} slope coefficients, and in situ reflectance data, we compared our predicted a_{CDOM} at 350 nm with the measured absorption coefficients for the same station. The nonzero intercepts of equations (8)–(10) make the determination of a_{CDOM} and the slope coefficient of a_{CDOM} less certain in clear waters, where the calculated absorbance values converge to the equation intercepts. However, the a_{CDOM} at 350 nm calculated using the slope coefficients agreed with the measured values to within 6–50% at various stations. We also compared our extrapolated a_{CDOM} at 300 nm with that predicted by the *Kahru and Mitchell* [2001] model. The two models agreed to within 10% in blue water, and 30–40% in coastal water.

4. Discussion

[24] The relationships between reflectance and K_d apply to all five cruises, over the whole summer in the Mid-Atlantic Bight, and in June in the Bering Sea (Figure 2). They describe variability over a wide range of water types, from turbid, inshore waters to clear, oligotrophic, offshore waters, although the Bering Sea samples seem to fall as a group somewhat lower in K_d (323 and 338 nm) than do the Mid-Atlantic Bight samples. The difference between the oceans may be the result of differences in the spectral backscattering and absorption ratios due to increased pigment packaging effects and/or a lower ratio of detrital to phytoplankton absorption in high-latitude than in midlatitude waters [e.g., *Mitchell*, 1992; *Reynolds et al.*, 2001]. The general relationships represent the central trends for the conditions in the regions considered. They will likely be widely applicable, although they require further testing in the winter and in other locations.

[25] The relationships between a_{CDOM} and K_d appear to be linear at 338 and 323 nm (Figure 3). (A linear relationship can also be applied to the data at 380 nm, but with less confidence.) Some of the scatter in Figure 3 might be due to the variety of times of day and latitudes at which the K_d measurements were made, which would change the geometry of the irradiance entering the water.

[26] K_d is not the same as total absorption. It depends on the geometric distribution of radiation, which is influenced by scattering, Sun angle and atmospheric conditions. The average cosine of downwelling irradiance, $\overline{\mu_d}$, is used to convert from $K_d(\lambda)$ to $a(\lambda)$ according to the following relation [*Kirk*, 1994]:

$$a(\lambda) = K_d(\lambda)\overline{\mu_d}(\lambda) \tag{18}$$

The relationships between a_{CDOM} and K_d presented in equations (8)–(10) show that if $\overline{\mu_d}$ in equation (18) were taken to be approximately 0.7 as is usual for visible radiation [see *Ciotti et al.*, 1999], a_{CDOM} would be greater than the total absorption coefficient calculated as $K_d(\lambda)\overline{\mu_d}(\lambda)$. (Table 2 shows that the slopes of equations (8)–(10) are significantly greater than 0.7.) Previous work has shown the same paradox [*Morris et al.*, 1995; *DeGrandpre et al.*, 1996; *Mitchell et al.*, 2002].

[27] Empirical and theoretical evidence suggests that $\overline{\mu_d}$ must be higher than the values normally used for diffuse visible radiation. Measurements with a HobiLabs HydroRad-4 in Lake Superior, where optical conditions are similar to those in the midshelf region of the Mid-Atlantic Bight, show that $\overline{\mu_d}$ is higher at shorter wavelengths and is 0.9 at 400 nm (A. Vodacek, personal communication, 2001). *Mitchell et al.* [2002] also found high values of $\overline{\mu_d}$ for UV radiation. This result is supported by theory. *Kirk* [1994] and *Bannister* [1992] show with Monte Carlo simulations that the asymptotic $\overline{\mu_d}$ increases as the ratio of scattering, $b(\lambda)$ (m^{-1}), to total absorption, $a(\lambda)$ (m^{-1}), decreases, and

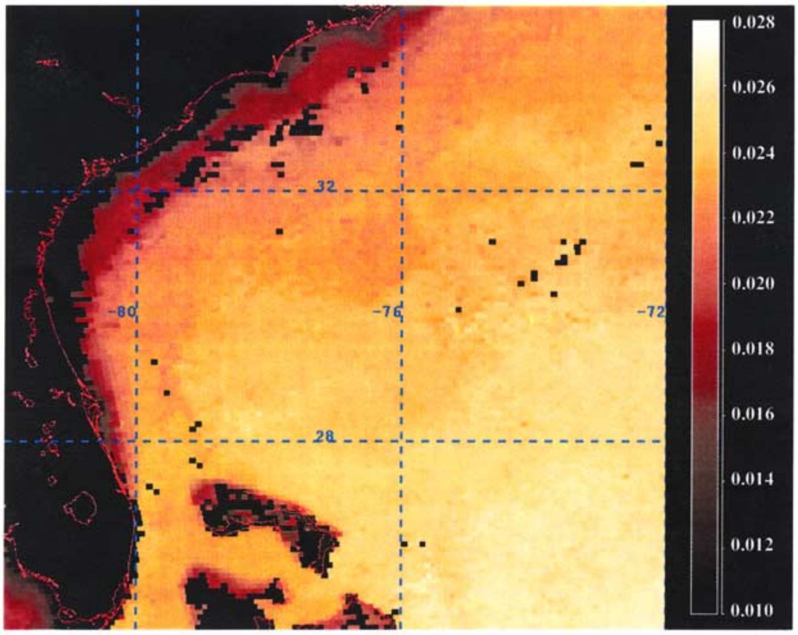

(a) January, 1999

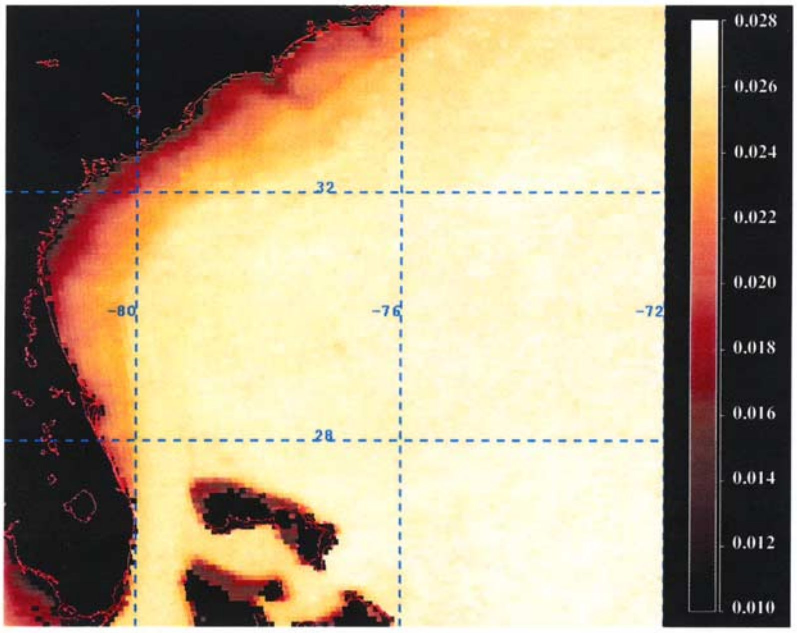

(b) July, 1999

Figure 6. Slope coefficient for CDOM absorption spectra (nm^{-1}) in the Georgia Bight, calculated from SeaWiFS normalized water-leaving radiance data, binned to 9 km × 9 km, monthly resolution: (a) January 1999 and (b) July 1999.

approaches 1 as $b(\lambda)/a(\lambda)$ approaches 0 for vertically incident light. The ratio $b(\lambda)/a(\lambda)$ must be lower for UV than for visible radiation: absorption increases exponentially (proportional to eλ)with decreasing wavelength, while scattering only increases (with decreasing wavelength) proportionally to wavelength to the power of 0–1 [*Gordon et al.*, 1988] or 2 [*Sathyendranath et al.*, 1989]. From *Bannister*'s [1992] model, a $\overline{\mu_d}$ of 0.9–0.97 for UV radiation is quite possible. The relationships between a_{CDOM} and K_d presented in equations (8)–(10) are consistent with this range of values of $\overline{\mu_d}$ for UV radiation. (Where individual values of $\overline{\mu_d}$ exceed 1, there must be an error associated with the absorption and/or K_d measurements, possibly due to wave focusing [e.g., *Zaneveld et al.*, 2001].)

[28] Accepting that $\overline{\mu_d}$ might be close to 1 for UV radiation, CDOM appears to absorb about 90% of the incident UV radiation (equations (8)–(10)) in the offshore samples. This does not seem unreasonable in the open ocean where most of the CDOM comes from the decomposition of phytoplankton [*Kalle*, 1966], the only other open ocean component whose UV absorption varies seasonally. In the Delaware and Chesapeake Bays, CDOM is responsible for much less of the total attenuation than it is offshore. Both bays are visibly turbid, so particles probably absorb and scatter much of the incident radiation.

[29] The variation among the ratios a_{CDOM}/K_d reported at 323, 338, and 380 nm requires some explanation. It might result from errors in the determination of K_d, wavelength-dependent variation of $\overline{\mu_d}$ or of the b/a ratio, or from absorption by other components, such as the photoprotective mycosporine-like amino acid pigments, MAAs. These pigments are produced by some phytoplankton and absorb most strongly between 300 and 360 nm [*Karentz et al.*, 1991; *Vernet and Whitehead*, 1996]. Interactions of this nature could represent a limitation to the remote determination of CDOM absorption coefficients, since, in a phytoplankton bloom which produces a high concentration of MAAs, the relationships developed above might not apply. The particularly high ratio of a_{CDOM} to K_d reported for 380 nm should be used with caution because of the low correlation coefficient of that relationship ($r^2 = 0.66$).

[30] Figure 4 shows a distinct seasonal change in UV attenuation. K_d at 323 nm appears to have decreased by about 50% from May to August. Overall, the areas of low attenuation seem to have moved northward. Both coastal and offshore areas became more transparent to UV throughout the summer, although it is not possible from these images to determine whether the change was due more to in situ photobleaching of water or to decreased terrestrial runoff. Attenuation at 338 and 380 nm follows the same pattern, as does the CDOM absorption coefficient (data not shown), which is tied directly to K_d in the equations used to generate the images. *Vodacek et al.* [1997] attributed a measured summertime decrease in surface layer absorbance by CDOM to photobleaching associated with prolonged shallow stratification of the surface layer. Increased penetration of UV combined with a shallowing of the surface mixed layer must result in higher exposures of phytoplankton and bacteria to UV in late summer.

[31] Figure 6 illustrates several points. As for K_d, the simple relationships derived in this work do not require the assumption of a single slope coefficient for all CDOM absorption spectra. There is a unique slope for every magnitude of the CDOM absorption coefficient at a given wavelength. The calculated slope coefficient of the log linearized CDOM absorption coefficient spectrum increases with distance from shore in the Georgia Bight (Figure 5), from about 0.014 nm^{-1} close to shore to about 0.028 nm^{-1} offshore, which is consistent with in situ measurements by *Vodacek et al.* [1997] (-0.01 to -0.034 nm^{-1} in the Mid-Atlantic Bight) and *Johannessen* [2000]. Seasonal changes are also apparent in this figure. In July the slope coefficient is generally higher than it is in January, and it increases more quickly and less smoothly with distance from shore. Our method cannot predict changes in slope coefficient independent of changes in the magnitude of UV attenuation. However, it is relevant that the higher slope coefficient offshore may be due to photobleaching, as suggested by *Vodacek et al.* [1997] for the Mid-Atlantic Bight. The more distinct zonation apparent in the July figure may relate to lower terrestrial runoff and increased stability of the water column, but it is difficult to ascertain the causes of the patterns in these remote measurements.

5. Conclusion

[32] The empirical relationships reported here may be used to calculate UV attenuation and CDOM absorption coefficients from remotely sensed visible reflectance data. The relationships specify an increase of the spectral slope coefficients for both attenuation and CDOM absorption as attenuation and absorption decrease, although the spectral slope coefficient of CDOM absorption should be used with caution in waters with low K_d. The empirical relationships we describe apply over a wide range of water types, in two oceans. Their application to the Mid-Atlantic Bight shows a distinct seasonal change in UV attenuation. The a_{CDOM} slope coefficient image produced for the Georgia Bight shows that they give reasonable remote estimates for this important optical property. The main uses of these relationships will probably be to correct chlorophyll algorithms, to calculate photochemical reaction rates, and to help determine where and when to study in situ changes in optical properties.

[33] **Acknowledgments.** We would like to thank R. F. Davis, C. Dempsey, R. J. Moore, J.-P. Parkhill, L. Ziolkowski, C. Fichot and the officers and crew of the *R/V Wecoma,* the *R/V Seward Johnson,* and the *R/V Cape Henlopen* for technical and computer assistance. Drs. J. Berwald, R. Zepp, A. Vodacek and Á. Ciotti, and Mr. Y. Huot provided useful discussions. We thank Dr. M. Lewis, M. MacDonald and K. Baith for help with the acquisition and manipulation of SeaWiFS data. We appreciate the constructive comments of four anonymous reviewers and Assistant Editor B. G. Mitchell. The SeaWiFS Project (Code 970.2) and the Distributed Active Archive Center (Code 902) at the Goddard Space Flight Center, Greenbelt, MD 20771, under the sponsorship of NASA's Mission to Planet Earth Program, produced and distributed the satellite data. NSERC in Canada and ONR-Environmental Optics in the United States provided funding for this research.

References

Aiken, J., G. F. Moore, and P. M. Holligan, Remote sensing of oceanic biology in relation to global climate change, *J. Phycol.*, *28*, 579–590, 1992.

Allard, B., H. Borén, C. Pettersson, and G. Zhang, Degradation of humic substances by UV irradiation, *Environ. Int.*, *20*, 97–101, 1994.

Austin, R. W., and T. J. Petzold, The determination of the diffuse attenuation coefficient of sea water using the coastal zone color scanner, in *Oceanography From Space*, edited by J. F. R. Gower, pp. 239–256, Plenum, New York, 1981.

Bannister, T. T., Model of the mean cosine of underwater radiance and estimation of underwater scalar irradiance, *Limnol. Oceanogr.*, *37*, 773–780, 1992.

Blough, N. V., and R. G. Zepp, Reactive oxygen species in natural waters, in *Active Oxygen in Chemistry*, edited by C. S. Foote et al., pp. 280–333, Chapman and Hall, New York, 1995.

Bricaud, A., A. Morel, and L. Prieur, Absorption by dissolved organic matter of the sea (yellow substance) in the UV and visible domains, *Limnol. Oceanogr.*, *26*, 43–55, 1981.

Bushaw, K. L., R. G. Zepp, M. A. Tarr, D. Schulz-Jander, R. A. Bourbonniere, R. E. Hodson, W. L. Miller, D. A. Bronk, and M. A. Moran, Photochemical release of biologically labile nitrogen from dissolved organic matter, *Nature*, *381*, 400–404, 1996.

Carder, K. L., R. G. Steward, G. R. Harvey, and P. B. Ortner, Marine humic and fulvic acids: Their effects on remote sensing of ocean chlorophyll, *Limnol. Oceanogr.*, *34*, 68–81, 1989.

Chen, Y., S. U. Khan, and M. Schnitzer, Ultraviolet irradiation of dilute fulvic acid solutions, *Soil Sci. Soc. Am. J.*, *42*, 292–296, 1978.
Ciotti, Á. M., J. J. Cullen, and M. R. Lewis, A semi-analytical model of the influence of phytoplankton community structure on the relationship between light attenuation and ocean color, *J. Geophys. Res.*, *104*, 1559–1578, 1999.
Cooper, W. J., R. G. Zika, R. G. Petasne, and A. M. Fischer, Sunlight-induced photochemistry of humic substances in natural waters: Major reactive species, in *Aquatic Humic Substances: Influence on Fate and Treatment of Pollutants*, edited by I. H. Suffet and P. McCarthy, pp. 332–362, Am. Chem. Soc., Washington, D. C., 1989.
Cullen, J. J., and P. J. Neale, Ultraviolet radiation, ozone depletion, and marine photosynthesis, *Photosynth. Res.*, *39*, 303–320, 1994.
Cullen, J. J., R. F. Davis, J. S. Bartlett, and W. L. Miller, Toward remote sensing of UV attenuation, photochemical fluxes, and biological effects of UV in surface waters, paper presented at Current and Emerging Issues in Aquatic Science: Aquatic Sciences Meeting, Am. Soc. of Limnol. and Oceanogr., Santa Fe, N. M., 1997.
DeGrandpre, M. D., A. Vodacek, R. K. Nelson, E. J. Bruce, and N. V. Blough, Seasonal seawater optical properties of the U. S. Middle Atlantic Bight, *J. Geophys. Res.*, *101*, 22,727–22,736, 1996.
Fenton, N., J. Priddle, and P. Tett, Regional variations in bio-optical properties of the surface waters in the Southern Ocean, *Antarctic Sci.*, *6*, 443–448, 1994.
Ferrari, G. M., M. D. Dowell, S. Grossi, and C. Targa, Relationship between the optical properties of chromophoric dissolved organic matter and total concentration of dissolved organic carbon in the southern Baltic Sea region, *Mar. Chem.*, *55*, 299–316, 1996.
Fraser, R. S., S. Mattoo, E.-N. Yeh, and C. R. McClain, Algorithm for atmospheric and glint corrections of satellite measurements of ocean pigment, *J. Geophys. Res.*, *102*, 17,107–17,118, 1997.
Gordon, H. R., and D. K. Clark, Clear water radiances for atmospheric correction of Coastal Zone Color Scanner imagery, *Appl. Opt.*, *20*, 4175–4180, 1981.
Gordon, H. R., D. K. Clark, J. W. Brown, O. B. Brown, R. H. Evans, and W. W. Broenkow, Phytoplankton pigment concentrations in the Middle Atlantic Bight: Comparison of ship determinations and CZCS estimates, *Appl. Opt.*, *22*, 20–36, 1983.
Gordon, H. R., O. B. Brown, R. H. Evans, J. W. Brown, R. C. Smith, K. S. Baker, and D. K. Clark, A semianalytic radiance model of ocean color, *J. Geophys. Res.*, *93*, 10,909–10,924, 1988.
Granéli, W., M. Lindell, and L. Tranvik, Photo-oxidative production of dissolved inorganic carbon in lakes of different humic content, *Limnol. Oceanogr.*, *41*, 698–706, 1996.
Gregg, W. W., and K. L. Carder, A simple spectral solar irradiance model for cloudless maritime atmospheres, *Limnol. Oceanogr.*, *35*, 1657–1675, 1990.
Hochman, H. T., F. E. Müller-Karger, and J. J. Walsh, Interpretation of the Coastal Zone Color Scanner signature of the Orinoco River plume, *J. Geophys. Res.*, *99*, 7443–7455, 1994.
Hoge, F. E., M. E. Williams, R. N. Swift, J. K. Yungel, and A. Vodacek, Satellite retrieval of the absorption coefficient of chromophoric dissolved organic matter in continental margins, *J. Geophys. Res.*, *100*, 24,847–24,854, 1995.
Højerslev, N. K., Spectral light absorption by Gelbstoff in coastal waters displaying highly different concentrations, paper presented at Ocean Optics XIV, Off. of Nav. Res., NASA, Honolulu, Hawaii, 1998.
Jeffrey, W. H., R. J. Pledger, P. Aas, S. Hager, R. Von Haven, and D. L. Mitchell, Diel and depth profiles of DNA photodamage in bacterioplankton exposed to ambient solar ultraviolet radiation, *Mar. Ecol. Prog. Ser.*, *137*, 283–291, 1996.
Jeffrey, W. H., J. P. Kase, and S. W. Wilhelm, UV radiation effects on heterotrophic bacterioplankton and viruses in marine ecosystems, in *The Effects of UV Radiation in the Marine Environment*, edited by S. de Mora, S. Demers, and M. Vernet, pp. 206–236, Cambridge Univ. Press, New York, 2000.
Johannessen, S. C., A photochemical sink for dissolved organic carbon in the ocean, Ph.D. diss., 176 pp., Dalhousie Univ., Halifax, N. S., Canada, 2000.
Johannessen, S. C., and W. L. Miller, Quantum yield for the photochemical production of dissolved inorganic carbon in seawater, *Mar. Chem.*, *76*, 271–283, 2001.
Kahru, M., and B. G. Mitchell, Empirical chlorophyll algorithm and preliminary SeaWiFS validation for the California Current, *Int. J. Remote Sens.*, *20*, 3423–3429, 1999.
Kahru, M., and B. G. Mitchell, Seasonal and nonseasonal variability of satellite-derived chlorophyll and colored dissolved organic matter concentration in the California Current, *J. Geophys. Res.*, *106*, 2517–2529, 2001.
Kaiser, E., and G. J. Herndl, Rapid recovery of marine bacterioplankton after inhibition by UV radiation in coastal waters, *Appl. Environ. Microbiol.*, *63*, 4026–4031, 1997.
Kalle, K., The problem of Gelbstoff in the sea, *Oceanogr. Mar. Biol. Annu. Rev.*, *4*, 91–104, 1966.
Karentz, D., F. S. McEuen, M. C. Land, and W. C. Dunlop, Survey of mycosporine-like amino acid compounds in Antarctic marine organisms: Potential protection from ultraviolet exposure, *Mar. Biol.*, *108*, 157–166, 1991.
Kettle, A. J., A model of the temporal and spatial distribution of carbon monoxide in the mixed layer, M. S. diss., Woods Hole Oceanogr. Inst., Woods Hole, Mass., 1994.
Kieber, D. J., J. McDaniel, and K. Mopper, Photochemical source of biological substrates in seawater: Implications for carbon cycling, *Nature*, *341*, 637–639, 1989.
Kirk, J. T. O., *Light and Photosynthesis in Aquatic Ecosystems*, Cambridge Univ. Press, New York, 1994.
Markager, S., and W. F. Vincent, Spectral light attenuation and the absorption of UV and blue light in natural waters, *Limnol. Oceanogr.*, *45*, 642–650, 2000.
Michaels, A. F., and D. A. Siegel, Quantification of non-algal light attenuation in the Sargasso Sea: Implications for biogeochemistry and remote sensing, *Deep Sea Res., Part II*, *43*, 321–345, 1996.
Miles, C. J., and P. L. Brezonik, Oxygen consumption in humic-colored waters by a photochemical ferrous-ferric catalytic cycle, *Environ. Sci. Technol.*, *15*, 1089–1095, 1981.
Miller, W. L., Effects of UV radiation on aquatic humus: Photochemical principles and experimental considerations, in *Aquatic Humic Substances: Ecology and Biochemistry*, edited by D. Hessen and L. Tranvik, pp. 125–143, Springer-Verlag, New York, 1997.
Miller, W. L., and D. Kester, Photochemical iron reduction and iron bioavailability in seawater, *J. Mar. Res.*, *52*, 325:343, 1994.
Miller, W. L., and R. G. Zepp, Photochemical production of dissolved inorganic carbon from terrestrial organic matter: Significance to the oceanic organic carbon cycle, *Geophys. Res. Lett.*, *22*, 417–420, 1995.
Mitchell, B. G., Predictive bio-optical relationships for polar oceans and marginal ice zones, *J. Mar. Syst.*, *3*, 91–105, 1992.
Mitchell, B. G., M. Kahru, J. Wieland, and M. Stramska, Determination of spectral absorption coefficients of particles, dissolved material and phytoplankton for discrete water samples, in *Ocean Optics Protocols for Satellite Ocean Color Sensor Validation, Revision 3*, *Volume 2*, edited by J. L. Muller and G. S. Fargion, *NASA Tech. Memo.*, *NASA/TM-2002-210004/Re3-Vol2*, 231–257, 2002.
Moore, C. A., C. T. Farmer, and R. G. Zika, Influence of Orinoco River water on hydrogen peroxide distribution and production in the eastern Caribbean, *J. Geophys. Res.*, *98*, 2289–2298, 1993.
Moore, R. J., Photochemical degradation of colored dissolved organic matter in two Nova Scotian lakes, M. S. diss., Dalhousie Univ., Halifax, N. S., Canada, 1999.
Mopper, K., and X. Zhou, Hydroxyl radical photoproduction in the sea and its potential impact on marine processes, *Science*, *250*, 661–664, 1990.
Mopper, K., X. Zhou, R. J. Kieber, D. J. Kieber, R. J. Sikorski, and R. D. Jones, Photochemical degradation of dissolved organic carbon and its impact on the oceanic carbon cycle, *Nature*, *353*, 60–62, 1991.
Moran, M. A., and R. G. Zepp, Role of photochemistry in the formation of biologically labile compounds from dissolved organic matter, *Limnol. Oceanogr.*, *42*, 1307–1316, 1997.
Morris, D. P., H. Zagarese, C. E. Williamson, E. G. Balseiro, B. R. Hargreaves, B. Mondenutti, R. Moeller, and C. Queimalinos, The attenuation of solar UV radiation in lakes and the role of dissolved organic carbon, *Limnol. Oceanogr.*, *40*, 1381–1391, 1995.
Nelson, N. B., Watching the world from above, in *Annual Report of the Bermuda Biological Station Research*, pp. 11–12, Bermuda Biol. Stn. Res., St. George's, 1997.
Reynolds, R. A., D. Stramski, and B. G. Mitchell, A chlorophyll-dependent semianalytical reflectance model derived from field measurements of absorption and backscattering coefficients within the Southern Ocean, *J. Geophys. Res.*, *106*, 7125–7138, 2001.
Sathyendranath, S., L. Prieur, and A. Morel, A three-component model of ocean color and its application to remote sensing of phytoplankton pigments in coastal waters, *Int. J. Remote Sens.*, *10*, 1373–1394, 1989.
Sikorski, R. J., and R. G. Zika, Modeling mixed-layer photochemistry of H_2O_2: Optical and chemical modeling of production, *J. Geophys. Res.*, *98*, 2315–2328, 1993a.
Sikorski, R. J., and R. G. Zika, Modeling mixed-layer photochemistry of H_2O_2: Physical and chemical modeling of distribution, *J. Geophys. Res.*, *98*, 2329–2340, 1993b.

Stedmon, C. A., S. Markager, and H. Kaas, Optical properties and signatures of chromophoric dissolved organic matter (CDOM) in Danish coastal waters, *Estuarine Coastal Shelf Sci.*, *51*, 267–278, 2000.
Vähätalo, A. V., M. Salkinoja-Salonen, P. Taalas, and K. Salonen, Spectrum of quantum yield for photochemical mineralization of dissolved organic carbon in a humic lake, *Limnol. Oceanogr.*, *45*, 664–676, 2000.
Valentine, R. L., and R. G. Zepp, Formation of carbon monoxide from the photodegradation of terrestrial dissolved organic carbon in natural waters, *Environ. Sci. Technol.*, *27*, 409–412, 1993.
Vernet, M., and K. Whitehead, Release of ultraviolet-absorbing compounds by the red-tide dinoflagellate *Lingulodinium polyhedra*, *Mar. Biol.*, *127*, 35–44, 1996.
Vodacek, A., F. Hoge, R. N. Swift, J. K. Yungel, E. T. Peltzer, and N. V. Blough, The use of in situ and airborne fluorescence measurements to determine UV absorption coefficients and DOC concentrations in surface waters, *Limnol. Oceanogr.*, *40*, 411–415, 1995.
Vodacek, A., N. V. Blough, M. D. DeGrandpre, E. T. Peltzer, and R. K. Nelson, Seasonal variation of CDOM and DOC in the Middle Atlantic Bight: Terrestrial inputs and photooxidation, *Limnol. Oceanogr.*, *42*, 674–686, 1997.
Zaneveld, J. R. V., E. Boss, and A. Barnard, Influence of surface waves on measured and modeled irradiance profiles, *Appl. Opt.*, *40*, 1442–1449, 2001.
Zhou, X., and K. Mopper, Determination of photochemically produced hydroxyl radicals in the sea and its potential impact on marine processes, *Mar. Chem.*, *30*, 71–88, 1990.

J. J. Cullen and W. L. Miller, Department of Oceanography, Dalhousie University, Halifax, Nova Scotia, Canada, B3H 4J1.
S. C. Johannessen, Institute of Ocean Sciences, 9860 W. Saanich Rd., P.O. Box 6000, Sidney, British Columbia, Canada V8L 4B2. (johannessen@pac.dfo-mpo.gc.ca)